The following Communications have been judged by at least two referees to be "very important papers" and will be published online at www.angewandte.org soon:

*K. Takahashi, M. Watanabe, T. Honda**
Highly Efficient Stereocontrolled Total Synthesis of (+)-Upial

Y. Tanaka, S. Saito, S. Mori, N. Aratani, H. Shinokubo, N. Shibata, Y. Higuchi, Z. S. Yoon, K. S. Kim, Su B. Noh, J. K. Park, D. Kim, A. Osuka**
Metalation of Expanded Porphyrins: A Chemical Trigger Used To Produce Molecular Twisting and Möbius Aromaticity

*I. Yoshikawa, J. Sawayama, K. Araki**
Highly Stable Giant Supramolecular Vesicles Composed of 2D Hydrogen-Bonded Sheet Assemblies of Guanosine Derivatives

*R. Cai, M. Sun, Z. Chen, R. Munoz, C. O Neill, D. Beving, Y. Yan**
Ionothermal Synthesis of Oriented Zeolite AEL Films and Their Application as Corrosion-Resistant Coatings

*Q. Wan, S. J. Danishefsky**
Free-Radical-Based, Specific Desulfurization of Cysteine: A Powerful Advance in the Synthesis of Polypeptides and Glycopolypeptides

*V. J. Sussman, J. E. Ellis**
From Storable Sources of Atomic Nb$^-$ and Ta$^-$ to Isolable Anionic Tris(1,3-butadiene)metal Complexes: [M(η^4-C_4H_6)$_3$]$^-$ (M=Nb, Ta)

News

Books

Highlights

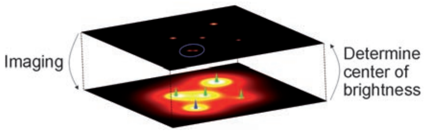

Zooming in: Ultrahigh-resolution microscopy is developing rapidly by different approaches. Photoactivation–localization microscopy (PALM) can now provide 3D images with fast acquisition times through the use of photoactivatable rhodamines and two-photon excitation. In PALM, individual emitters can be localized with nanometer precision simply by determining the centroid of the emission distribution.

Microscopy

Minireviews

Folding sheets: Organizing polymers with the help of β-sheet peptides is an emerging field of polymer research. The peptides employed to date range from linear and cyclic α peptides to fully synthetic peptide analogues. Nature's most basic lesson of secondary structure formation has been learned. Predicting the higher levels of hierarchical organization of peptide–copolymer aggregates will be the topic of the many lessons to come.

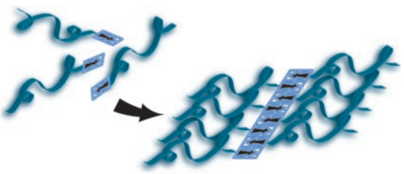

Peptide–Polymer Hybrids

Contents

Reviews

Supramolecular Chemistry

G. R. Desiraju* ______ **8342 – 8356**

Crystal Engineering: A Holistic View

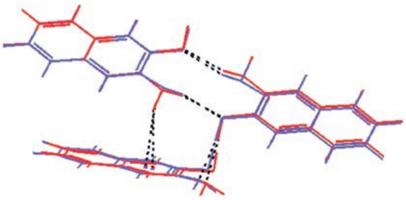

A crystal structure is a complex convolution of molecular structure and is hard to predict. Crystals are formed under thermodynamic or kinetic control. This dichotomy leads to polymorphism and further difficulties. This review surveys some recent challenges in the design of functional solid-state molecular materials. The picture shows experimental and computer-predicted crystal structures for 3-amino-2-naphthol.

Communications

VIP

Molecular Solar Cells

J.-J. Cid, J.-H. Yum, S.-R. Jang, M. K. Nazeeruddin,* E. Martínez-Ferrero, E. Palomares, J. Ko, M. Grätzel, T. Torres* ______ **8358 – 8362**

Molecular Cosensitization for Efficient Panchromatic Dye-Sensitized Solar Cells

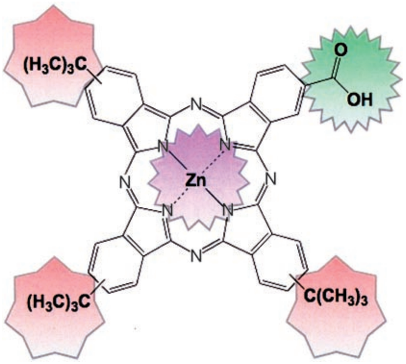

Dyeing together: An efficient panchromatic dye-sensitized solar cell is constructed by using a "molecular cocktail" composed of an organic dye and a zinc phthalocyanine (see picture). The use of multiple, complementary dyes (cosensitization) is an important step towards solar cells that operate across the full spectrum of solar irradiation.

VIP

Anisotropic Nanostructures

R. Klajn, A. O. Pinchuk, G. C. Schatz, B. A. Grzybowski* ______ **8363 – 8367**

Synthesis of Heterodimeric Sphere–Prism Nanostructures via Metastable Gold Supraspheres

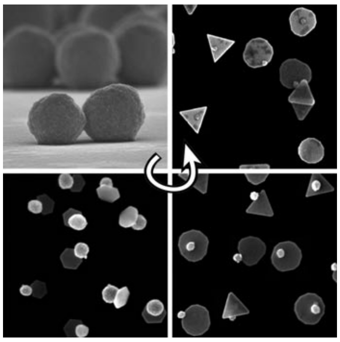

Changing shapes: Metastable spherical aggregates of gold nanoparticles undergo a one-to-one, thermally induced transformation into heterodimers comprising connected plate and spherical domains. By controlling the reaction time, it is possible to isolate a variety of structures differing in the relative sizes of the domains and in the overall optical properties (see picture).

For the USA and Canada: ANGEWANDTE CHEMIE International Edition (ISSN 1433-7851) is published weekly by Wiley-VCH, PO Box 191161, 69451 Weinheim, Germany. Air freight and mailing in the USA by Publications Expediting Inc., 200 Meacham Ave., Elmont, NY 11003. Periodicals postage paid at Jamaica, NY 11431. US POSTMASTER: send address changes to *Angewandte Chemie*, Wiley-VCH, 111 River Street, Hoboken, NJ 07030. Annual subscription price for institutions: US$ 7225/6568 (valid for print and electronic / print or electronic delivery); for individuals who are personal members of a national chemical society prices are available on request. Postage and handling charges included. All prices are subject to local VAT/ sales tax.

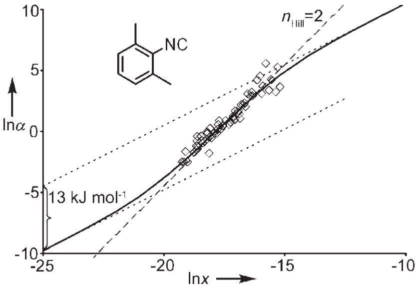

Two is better than one: Fe^{II} complexes of new porphyrins exist as dimers that bind small ligands cooperatively, as illustrated by the sigmoidal binding curve (fractional occupancy of binding sites, α, versus free-ligand concentration, x) for isocyanide $Me_2C_6H_3NC$. An allosteric interaction energy of up to 13 kJ mol^{-1}—comparable to that of hemoglobin—is achieved in a simple structural motif.

Allosteric Receptors

D. Khvostichenko, Q. Yang,
R. Boulatov* ______ **8368 – 8370**

Simple Heme Dimers with Strongly Cooperative Ligand Binding

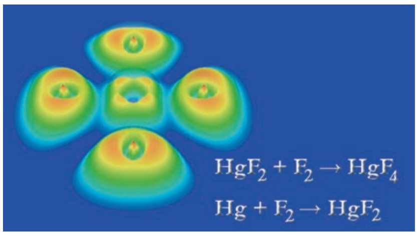

A new take on quicksilver: The elements of Group 12 are generally considered post-transition metals with filled d shells. However, calculations predict d^8 HgF_4 (see plot of the electron localization function) to be stable. IR spectroscopy in solid neon and argon matrixes gives first experimental evidence for HgF_4. As Hg^{IV}, mercury would be a true transition metal that fully utilizes its 5d orbitals in bonding.

High Oxidation States

VIP

X. Wang, L. Andrews,* S. Riedel,
M. Kaupp* ______ **8371 – 8375**

Mercury Is a Transition Metal: The First Experimental Evidence for HgF_4

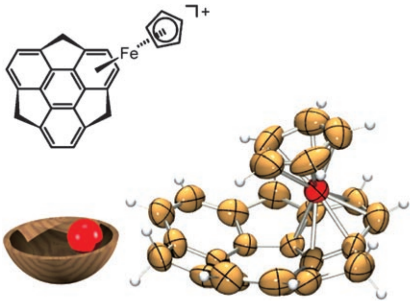

Dished up: The selective synthesis of a concave-bound iron complex was achieved by ligand exchange of a cyclopentadienyl ring of ferrocene with a fullerene-fragment π bowl, sumanene (see picture). The concave π surface serves as an η^6 ligand.

π-Bowl Complexes

VIP

T. Amaya, H. Sakane,
T. Hirao* ______ **8376 – 8379**

A Concave-Bound CpFe Complex of Sumanene as a Metal in a π Bowl

---

Spinning a magical web: The combination of fast magic-angle spinning, isotopic dilution, and high magnetic field yields particularly well-resolved solid-state ^{1}H NMR spectra, which are efficiently utilized to solve protein structure. New techniques are demonstrated, requiring only three days of data collection, to assign the proton signals and solve a high-resolution structure of microcrystalline GB1.

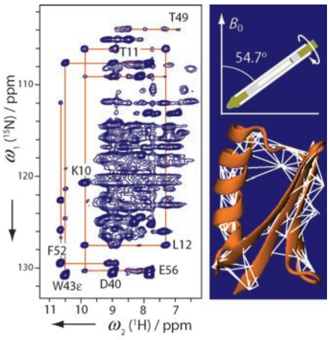

Protein NMR Spectroscopy

D. H. Zhou, J. J. Shea, A. J. Nieuwkoop,
W. T. Franks, B. J. Wylie, C. Mullen,
D. Sandoz, C. M. Rienstra* **8380 – 8383**

Solid-State Protein-Structure Determination with Proton-Detected Triple-Resonance 3D Magic-Angle-Spinning NMR Spectroscopy

May the force be with you: "Mirror-image" hairpin polyamides distinguish the L enantiomer of DNA (L-DNA) in the presence of natural DNA (D-DNA). This specificity is investigated by a molecular force balance at a single-molecule level. The "DNA balance" allows the measurement of rupture forces of match/mismatch diastereomeric complexes in a single experiment.

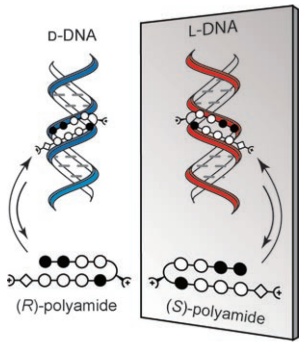

DNA Force Analysis

C. Dose, D. Ho, H. E. Gaub, P. B. Dervan,* C. H. Albrecht* ———— **8384 – 8387**

Recognition of "Mirror-Image" DNA by Small Molecules

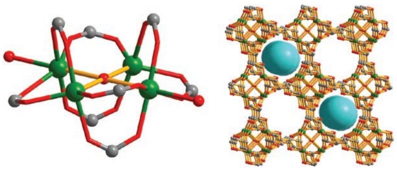

The zeolite way: Templating on charged organic species, which have long been used for synthesizing aluminosilicate zeolites, is shown to allow the self-assembly of enantiopure chiral molecular precursors into extended homochiral frameworks (see picture; Cd green, O red, C gray; the sky-blue spheres illustrate the open regions in the channels).

Metal–Organic Frameworks

J. Zhang, R. Liu, P. Feng, X. Bu* ———— **8388 – 8391**

Organic Cation and Chiral Anion Templated 3D Homochiral Open-Framework Materials with Unusual Square-Planar $\{M_4(OH)\}$ Units

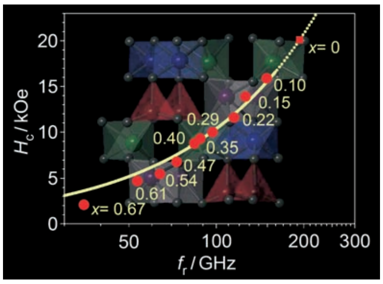

Restraining electromagnetic interference in the millimeter-wave region has been accomplished with a new electromagnetic absorber composed of ε-$Ga_xFe_{2-x}O_3$ ($0.10 \leq x \leq 0.67$) nanomagnets, which shows a ferromagnetic resonance in the range 35–147 GHz. The possibility that the ferromagnetic resonance can achieve a frequency of 190 GHz at $x \rightarrow 0$ is also suggested. See picture: H_c = coercive field; f_r = ferromagnetic resonance frequency.

Magnetic Materials

S. Ohkoshi,* S. Kuroki, S. Sakurai, K. Matsumoto, K. Sato, S. Sasaki ———— **8392 – 8395**

A Millimeter-Wave Absorber Based on Gallium-Substituted ε-Iron Oxide Nanomagnets

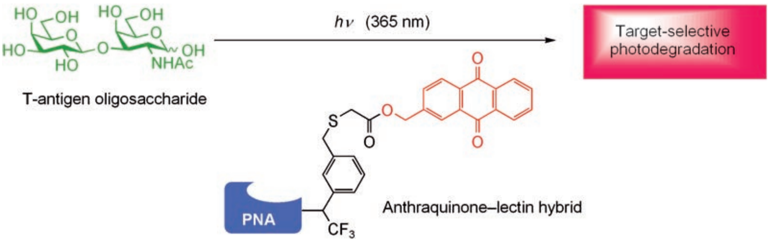

An innovative method for target-selective degradation of oligosaccharides induced by a light-activated hybrid molecule consisting of anthraquinone and lectin has been developed (see scheme). The reaction takes place under neutral conditions, and no additives are required. PNA = peanut agglutinin.

Oligosaccharides

M. Ishii, S. Matsumura, K. Toshima* ———— **8396 – 8399**

Target-Selective Degradation of Oligosaccharides by a Light-Activated Small-Molecule–Lectin Hybrid

Molecular Motors

W. Shi, M. I. Giannotti, X. Zhang,
M. A. Hempenius, H. Schönherr,
G. J. Vancso* ______ **8400 – 8404**

Closed Mechanoelectrochemical Cycles of Individual Single-Chain Macromolecular Motors by AFM

Motor cycles: Mechanoelectrochemical loops of single-chain macromolecular motors based on individual end-grafted poly(ferrocenyldimethylsilane) are shown by AFM to have an efficiency of up to 26 %. Upon oxidation of a prestretched chain, the chain length increases and the force decreases significantly as a result of intramolecular electrostatic repulsion between oxidized ferrocene units (see picture).

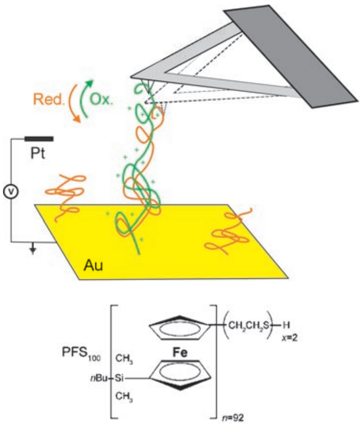

Biomineralization

M. Sumper,* R. Hett, G. Lehmann,
S. Wenzl ______ **8405 – 8408**

A Code for Lysine Modifications of a Silica Biomineralizing Silaffin Protein

A mass of codes: Lysine-rich silaffin proteins from diatoms guide silica formation by self-assembly processes. Aided by mass spectrometry, the analysis of 28 posttranslationally modified lysine residues in silaffin-3 from *Thalassiosira pseudonana* uncovers an amino acid sequence based code selecting the type of modification. This code may be a key element in the genetic control of species-specific silica architectures.

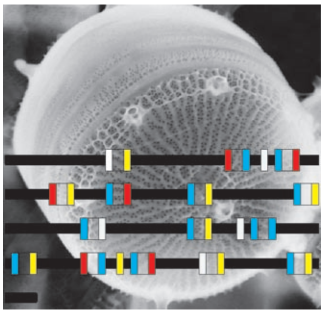

Supramolecular Chemistry

C. Arnal-Hérault, A. Pasc, M. Michau,
D. Cot, E. Petit, M. Barboiu* **8409 – 8413**

Functional G-Quartet Macroscopic Membrane Films

Transport systems: Long-range amplification of G-quadruplex self-organization by K$^+$ ion templating into double dynameric macroscopic films is described. The ordered membrane films (see image) contribute to fast electron/proton or Na$^+$/K$^+$ transport by the formation of directional conduction pathways.

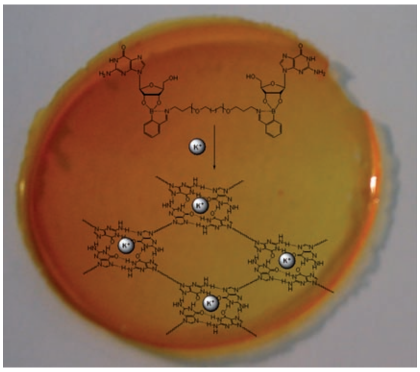

Directed Evolution

R. Fasan, M. M. Chen, N. C. Crook,
F. H. Arnold* ______ **8414 – 8418**

Engineered Alkane-Hydroxylating Cytochrome P450$_{BM3}$ Exhibiting Nativelike Catalytic Properties

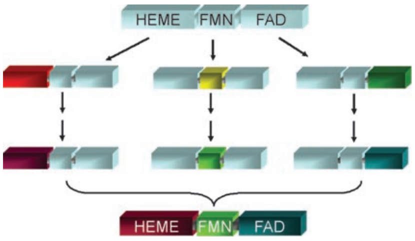

Divide, evolve, and conquer: A domain-based strategy (see scheme) was used to engineer high catalytic and coupling efficiency for propane hydroxylation in a multidomain cytochrome P450 enzyme. The engineered enzymes exhibit high total activities in whole-cell bioconversions of propane to propanol under mild conditions, using air as oxidant.

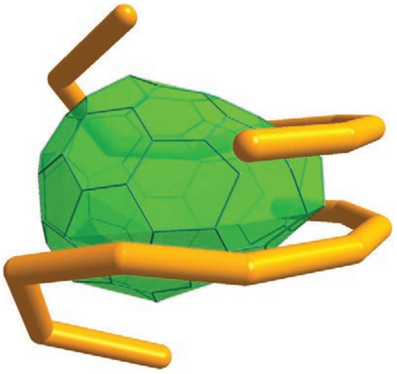

A chiral fullerene: The first ordered crystal structure of a derivative of the D_2-symmetric C_{76} fullerene, $C_{76}Cl_{18}$, is determined. The distorted carbon skeleton of $C_{76}Cl_{18}$ contains elongated C–C bonds and a unique π system. The C_{76} cage (see picture; green) is surrounded by two helical belts of chlorine atoms (orange).

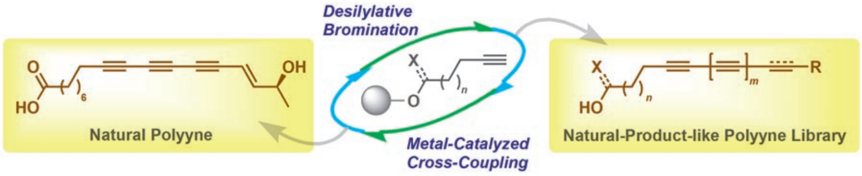

High in polyunsaturates: The combinatorial synthesis of a 65-membered polyyne library has been achieved by using an iterative acetylene homologation strategy combined with a solid support (see scheme). The library was evaluated against cancer cells to demonstrate its possible utility as a chemical tool to unravel cellular processes or as a platform for drug discovery and design.

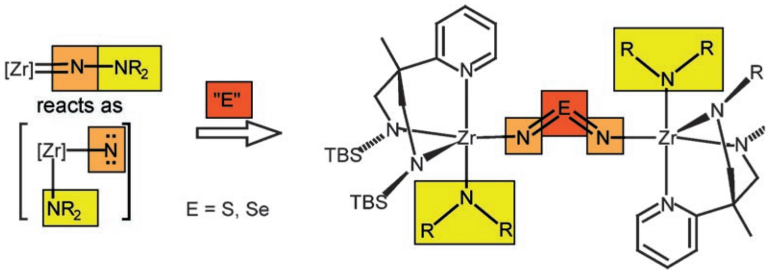

Piece by piece: Hydrazides at zirconium centers undergo facile N–N bond cleavage and react as equivalents for metallanitrenes, thus allowing the atom-by-atom assembly of bridging dinitridosulfate(IV) and dinitridoselenate(IV) ligands (see scheme; TBS = tBuMe$_2$Si).

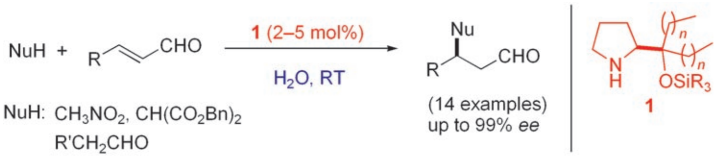

A pool of water-compatible catalysts, namely the chiral prolinol-based catalysts **1**, has been developed for highly enantioselective C–C bond-forming Michael reactions in water (see scheme). The synthesis of (*S*)-Rolipram, a type IV phosphodiesterase inhibitor, was also demonstrated.

Core–Shell Nanostructures

C. Xue, J. E. Millstone, S. Li,
C. A. Mirkin* ———— **8436 – 8439**

Plasmon-Driven Synthesis of Triangular Core–Shell Nanoprisms from Gold Seeds

Outside silver, inside gold: Gold nanoparticles are used as seeds to probe the role of plasmon excitation in the photomediated growth of silver nanoprisms. This approach generates novel core–shell nanostructures that contain a spherical (see TEM image, inset shows side view) or triangular-prism gold core with a triangular silver prism shell. The architecture of these particles can be tuned by controlling the excitation wavelength and gold-core diameter.

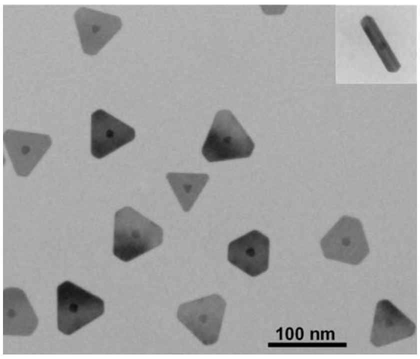

Cycloaddition

V. Aureggi, G. Sedelmeier* _ **8440 – 8444**

1,3-Dipolar Cycloaddition: Click Chemistry for the Synthesis of 5-Substituted Tetrazoles from Organoaluminum Azides and Nitriles

Cheap and safe: Conventional methods to prepare tetrazoles employ dangerous, toxic reagents. A new route to these heterocycles (see scheme) uses inexpensive and nontoxic dialkyl aluminum azides. The cycloaddition occurs under mild conditions and tolerates a variety of functional groups. The low cost and ecocompatibility make this process attractive for large-scale preparation.

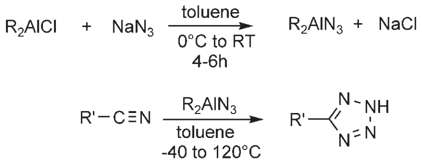

Fluorescent Probes

W. Jiang, Q. Fu, H. Fan, J. Ho,
W. Wang* ———— **8445 – 8448**

A Highly Selective Fluorescent Probe for Thiophenols

A rapid response to thiophenols is obtained with probe **1** (see scheme), which induces a significant (>50-fold) fluorescence enhancement as a result of cleavage of the electron-withdrawing moiety, thus generating strongly fluorescent molecule **2**. No fluorescence is obtained with aliphatic thiols, including cysteine and glutathione, or other nucleophiles.

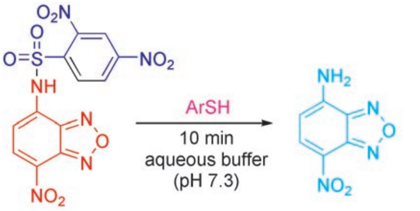

nonfluorescent (**1**)   strongly fluorescent (**2**)

Layered Compounds

Y. Ide, M. Ogawa* ———— **8449 – 8451**

Interlayer Modification of a Layered Titanate with Two Kinds of Organic Functional Units for Molecule-Specific Adsorption

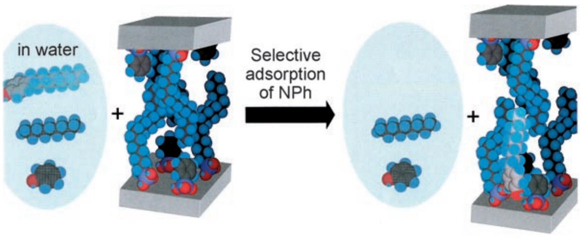

Selective removal: Alkyl and phenyl groups were immobilized within an interlayer space of a layered titanate to adsorb selectively and effectively 4-nonylphenol (NPh, in light colors) from aqueous solution. The immobilization of two kinds of functional units in a confined nanospace is a useful way to tailor materials with molecular recognition abilities for a wide variety of molecules.

Enzyme Catalysis

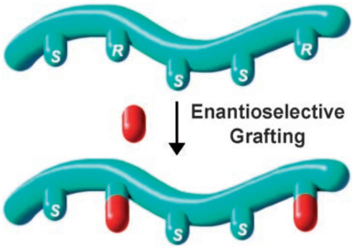

A programmed response: Enzyme-responsive materials have been prepared from enzymatically synthesized, enantiomerically pure monomers. The extent of the material's response is encoded within its chiral makeup. This code can be effectively read out by an enzymatic process, which leads to a change in the thermal properties of the material. The picture shows esterification of chiral alcohol groups on a polymer backbone (green) with vinyl acetate (red).

Enzyme Mechanisms

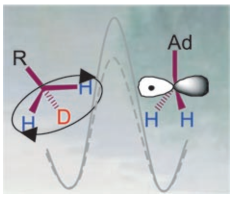

Intramolecular competition between hydrogen and deuterium atoms at the methyl group of methylaspartate was used to measure the intrinsic primary deuterium isotope effect for 5′-deoxyadenosine formation in a B_{12} enzyme. The value is much smaller than expected based on measurements on other B_{12} enzymes and model systems. This strongly suggests that glutamate mutase modulates the transition state for hydrogen transfer.

Carbonylation

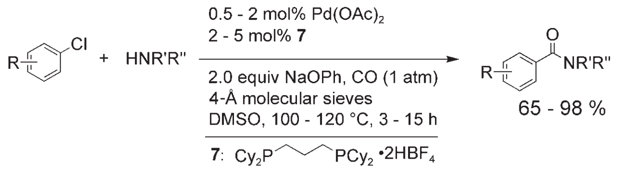

No pressure, no worries: A general, functional-group-tolerant, mild system for the Pd-catalyzed carbonylation of aryl chlorides to the corresponding amides has been developed. The catalyst operates at 1 atm CO using an inexpensive, air-stable, and commercially available ligand (see scheme, Cy = cyclohexyl). Sodium phenoxide is a critical additive in this transformation; its role has been studied using in situ IR spectroscopy.

Natural Products

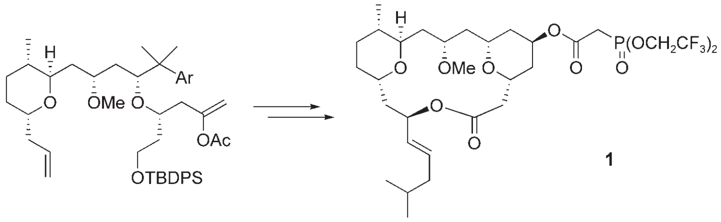

Oxidation leads to macrolactone: Oxidative carbon–carbon bond activation is a key step in the formal synthesis of leucascandrolide A, which is formed in one step from **1**. Additional features are stereoselective $BiBr_3$-mediated allylation, acetal formation as a fragment-coupling reaction, and a rhenium-mediated allylic alcohol transposition leading to stable macrolactol formation.

Contents

Asymmetric Catalysis

J. Wang, X. Hu, J. Jiang, S. Gou, X. Huang, X. Liu, X. Feng* ______ **8468 – 8470**

Asymmetric Activation of *tropos* 2,2′-Biphenol with Cinchonine Generates an Effective Catalyst for the Asymmetric Strecker Reaction of *N*-Tosyl-Protected Aldimines and Ketoimines

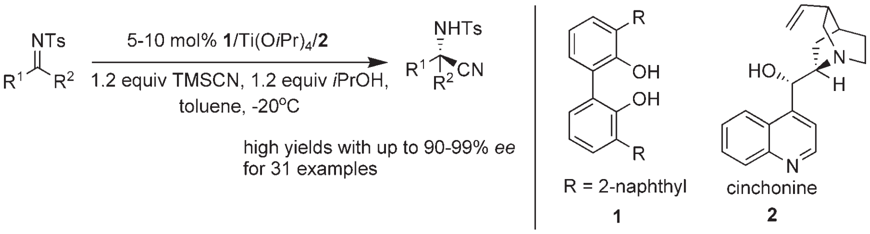

Tropo' bello! Asymmetric activation of *tropos* biphenol **1** and Ti(O*i*Pr)$_4$ with cinchonine **2** generates a remarkably effective catalyst in situ for the asymmetric Strecker reaction of *N*-tosyl (Ts) imines under mild conditions. Various substrates including aldimines, aryl alkyl ketoimines, and unsymmetrical diaryl ketoimines were investigated, and most of them exhibited high enantioselectivities (up to 99% *ee*) as well as high reactivities.

Asymmetric Catalysis

Y. Zhao, A. W. Mitra, A. H. Hoveyda,* M. L. Snapper* ______ **8471 – 8474**

Kinetic Resolution of 1,2-Diols through Highly Site- and Enantioselective Catalytic Silylation

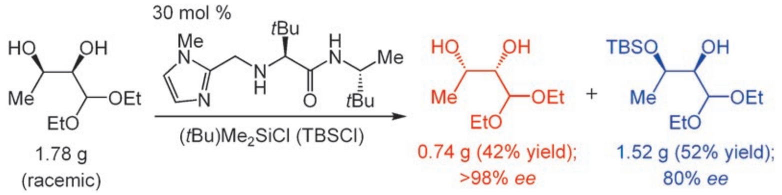

Resolved to silylate: A chiral silylation catalyst is used for kinetic resolution of three classes of acyclic 1,2-diols. The catalyst differentiates, with excellent precision, between the two hydroxy groups of a substrate. The majority of the diols, obtained in high enantiomeric purity, cannot be accessed with similar stereochemical purity through catalytic asymmetric dihydroxylation.

Chirality

S.-T. Wu, Y.-R. Wu, Q.-Q. Kang, H. Zhang, L.-S. Long,* Z. Zheng,* R.-B. Huang, L.-S. Zheng ______ **8475 – 8479**

Chiral Symmetry Breaking by Chemically Manipulating Statistical Fluctuation in Crystallization

Breaking out: By introducing a relatively stable intermediate to chemically control the nucleation rate, chiral symmetry breaking was achieved in the crystallization of intrinsically chiral helical coordination polymers. The fewer crystal clusters formed, the more pronounced the symmetry breaking (see picture).

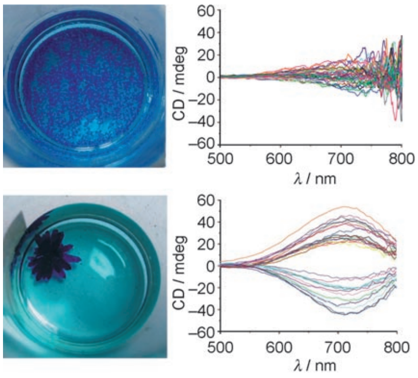

Conjugated Polymers

M. S. Taylor, T. M. Swager* **8480 – 8483**

Poly(anthrylenebutadiynylene)s: Precursor-Based Synthesis and Band-Gap Tuning

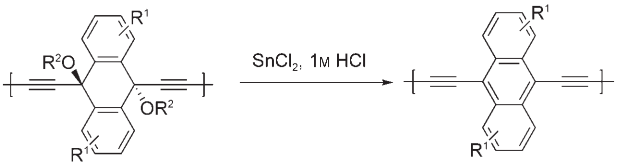

Skipping the monomer: A highly efficient reductive aromatization reaction transforms an unconjugated precursor polymer into a high-molecular-weight, butadiyne-linked anthracene homopolymer (see scheme). Photophysical and electrochemical analyses reveal that some of these new materials display remarkable stability in both neutral and doped states and have unusually low intrinsic band gaps.

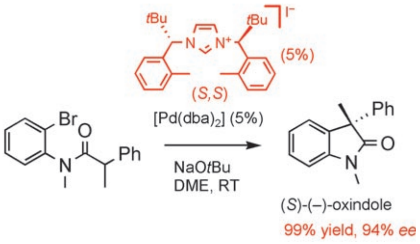

Bring on the big cats: New, C_2-symmetric bulky N-heterocyclic carbene ligands bring major improvements in the palladium-catalyzed asymmetric intramolecular α-arylation of amides to give oxindoles (see picture, dba = *trans*,*trans*-dibenzylideneacetone), which are formed in high yield and excellent enantiomeric purity.

Asymmetric Catalysis

E. P. Kündig,* T. M. Seidel, Y. Jia,
G. Bernardinelli ________ **8484 – 8487**

Bulky Chiral Carbene Ligands and Their Application in the Palladium-Catalyzed Asymmetric Intramolecular α-Arylation of Amides

Off-center: The material NaI_3O_8 is obtained as millimeter-sized single crystals (see photograph of a single crystal; crystal size: 2 × 2 × 5 mm^3), and its crystal structure is acentric. It is transparent up to 12.5 μm, thus covering the three atmospheric transparency windows. It generates an intense second-harmonic-generation signal and has a high optical damage threshold.

Nonlinear Optics

D. Phanon,
I. Gautier-Luneau* ________ **8488 – 8491**

Promising Material for Infrared Nonlinear Optics: NaI_3O_8 Salt Containing an Octaoxotriiodate(V) Anion Formed from Condensation of $[IO_3]^-$ Ions

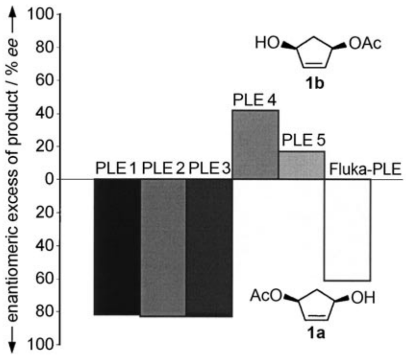

An esterase toolbox: A set of isoenzymes of pig liver esterases (PLE) is identified, cloned, and overexpressed in *E. coli*. They show striking differences in enantioselectivity and enantiopreference in the kinetic resolution of acetates of secondary alcohols as well as the desymmetrization of *cis*-3,5-diacetoxycyclopent-1-ene to **1a** and **1b** (see picture: enantiopreference of the new isoenzymes and a commercial PLE isoenzyme mixture).

Enzyme Catalysis

A. Hummel, E. Brüsehaber, D. Böttcher,
H. Trauthwein, K. Doderer,
U. T. Bornscheuer* ________ **8492 – 8494**

Isoenzymes of Pig-Liver Esterase Reveal Striking Differences in Enantioselectivities

A time-resolved study of magnetite formation in magnetotactic bacteria has shown that magnetite biomineralization proceeds first by coprecipitation of Fe^{2+} and Fe^{3+} ions and then via small magnetite crystallites (see picture) within invaginating magnetosomes associated with the cell membrane, which further develop into mature crystals after magnetosome vesicles are released from the cell membrane.

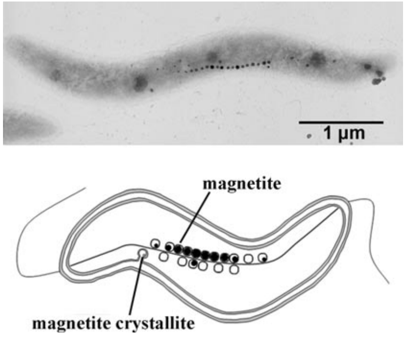

Biomineralization

D. Faivre, L. H. Böttger, B. F. Matzanke,
D. Schüler* ________ **8495 – 8499**

Intracellular Magnetite Biomineralization in Bacteria Proceeds by a Distinct Pathway Involving Membrane-Bound Ferritin and an Iron(II) Species

Contents

Homogeneous Catalysis

G. Hilt,* J. Treutwein ______ **8500 – 8502**

Cobalt-Catalyzed Alder–Ene Reaction

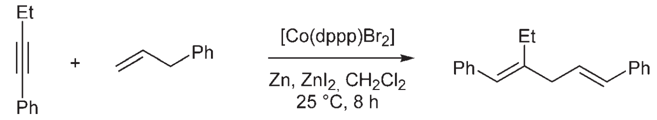

Next reactant, new pathway: An inexpensive cobalt–diphosphine complex is able to catalyze the intermolecular Alder–ene reaction of internal alkynes with terminal alkenes. The products are functionalized 1,4-dienes (see scheme) which are obtained in good yields and with excellent chemo-, regio-, and stereoselectivities.

Boron Clusters

E. Oger, N. R. M. Crawford, R. Kelting,
P. Weis,* M. M. Kappes,*
R. Ahlrichs* ______ **8503 – 8506**

Boron Cluster Cations: Transition from Planar to Cylindrical Structures

Above a certain size, boron clusters prefer a cylindrical arrangement over a planar one. Experimental determination of the collision cross section combined with density functional calculations showed that the transition to cylindrical structures takes place at B$_{16}^+$ for boron clusters. The picture shows some of the investigated structures. The left column represents the global minima; the other columns show less favorable structures.

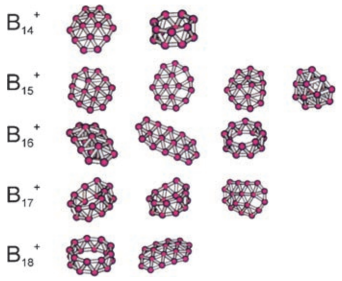

Oligomerization Catalysis

B. Lian, K. Beckerle, T. P. Spaniol,
J. Okuda* ______ **8507 – 8510**

Regioselective 1-Hexene Oligomerization Using Cationic Bis(phenolato) Group 4 Metal Catalysts: Switch from 1,2- to 2,1-Insertion

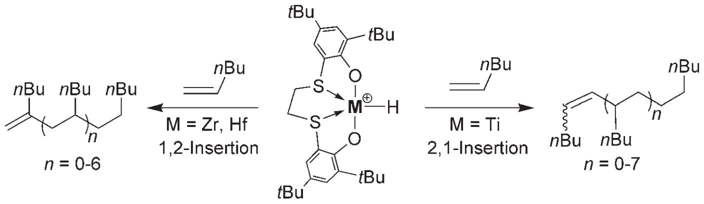

A cat of two tales: Cationic Group 4 metal catalysts that contain a linked bis(phenolato) ligand efficiently catalyze the oligomerization of 1-hexene. Whereas oligo(1-hexene)s arising from 2,1-insertion of 1-hexene are observed for the titanium complexes, those prepared using zirconium and hafnium complexes are formed by 1,2-insertion.

Drug Design

C. Gerlach, M. Smolinski, H. Steuber,
C. A. Sotriffer, A. Heine, D. G. Hangauer,
G. Klebe* ______ **8511 – 8514**

Thermodynamic Inhibition Profile of a Cyclopentyl and a Cyclohexyl Derivative towards Thrombin: The Same but for Different Reasons

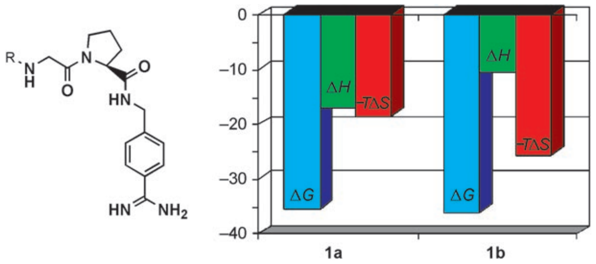

Small changes, big effects: Two thrombin inhibitors (see picture; R = cyclopentyl (**1a**), R = cyclohexyl (**1b**)) were characterized thermodynamically and computationally to explain their identical binding constants. Surprisingly, the free energy of binding is achieved with different enthalpic and entropic contributions (see plot).

Supporting information is available on the WWW (see article for access details).

A video clip is available as Supporting Information on the WWW (see article for access details).

Service


CHEMMEDCHEM
CHEMISTRY ENABLING DRUG DISCOVERY
Inexpensive
Available in two steps
10/2007
WILEY-VCH